Reversible and irreversible temperature-induced changes in exchange-biased planar Hall effect bridge (PHEB) magnetic field sensors

G. Rizzi, N.C. Lundtoft, F.W. Østerberg, M.F. Hansen*

Department of Micro- and Nanotechnology, Technical University of Denmark
DTU Nanotech, Building 345B, DK-2800 Kongens Lyngby, Denmark
*Mikkel.Hansen@nanotech.dtu.dk

ABSTRACT

We investigate the changes of planar Hall effect bridge magnetic field sensors upon exposure to temperatures between 25°C and 90°C. From analyses of the sensor response vs. magnetic fields we extract the exchange bias field $H_{\rm ex}$, the uniaxial anisotropy field $H_{\rm K}$ and the anisotropic magnetoresistance (AMR) of the exchange biased thin film at a given temperature and by comparing measurements carried out at elevated temperatures T with measurements carried out at 25°C after exposure to T, we can separate the reversible from the irreversible changes of the sensor. The results are not only relevant for sensor applications but also demonstrate the method as a useful tool for characterizing exchange-biased thin films.

Keywords: Magnetic biosensors, Planar Hall effect, Exchange bias, anisotropic magnetoresistance

1 INTRODUCTION

For applications of any sensor, it is important to know and, if needed, correct for the effect of varying temperatures of the sensor environment to be able to perform reliable measurements. We are investigating exchange-biased planar Hall effect sensors for magnetic biodetection [1, 2]. This sensing principle is attractive due to its low intrinsic noise and potentially high signal-to-noise [3].

Here, we systematically study the changes of the response of planar Hall effect bridge sensors [4] when these are exposed to temperatures between 25°C and 90°C corresponding to the temperatures typically employed in DNA based assays with amplification by the polymerase chain reaction (PCR). From analyses of sensor signal in sweeping magnetic field we extract the thin film parameters of the sensor stack at all investigated temperatures and by performing measurements at 25°C after all measurements at elevated temperatures we can quantify and distinguish reversible and irreversible changes of each of the sensor parameters. The results are generally relevant for applications of exchange-biased thin film sensors and demonstrate the method as a general tool for studying thin film properties vs. temperature.

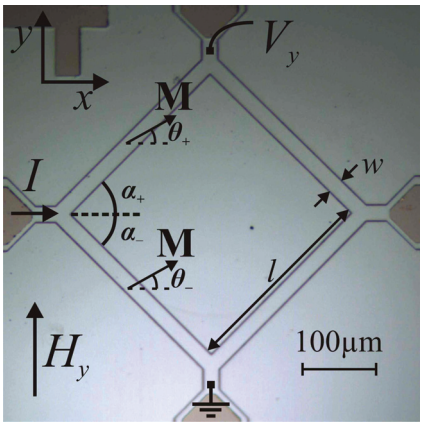

Figure 1: Image of planar Hall effect bridge (PHEB) sensor with definitions of sensor geometry and variables.

2 SENSOR MODEL

We consider a material exhibiting anisotropic magnetoresistance (AMR) such that the electrical resistivities $\rho_\parallel$ and $\rho_\perp$ parallel and perpendicular to the magnetization $\mathbf{M}$ differ and give rise to the AMR ratio $\Delta\rho/\rho_{\rm av}$ where $\Delta\rho \equiv \rho_\parallel - \rho_\perp$ and $\rho_{\rm av} \equiv \frac{1}{3}\rho_\parallel + \frac{2}{3}\rho_\perp$. For permalloy ($Ni_{80}Fe_{20}$), $\Delta\rho/\rho_{\rm av} \approx$ 2-3%. Figure 1 shows a Wheatstone bridge consisting of four segments, each forming an angle α to the x-axis and having a homogeneous magnetization forming an angle θ to the x-axis. The resistance of an element of length l, width w and thickness t is [4]

$$R(\alpha,\theta) = \frac{l}{wt}\left[\tfrac{1}{2}(\rho_\parallel + \rho_\perp) - \tfrac{1}{2}\Delta\rho\cos\left[2(\theta-\alpha)\right]\right]. \quad (1)$$

In Figure 1, four pairwise identical elements are combined to form a Wheatstone bridge. A current I injected in the x-direction gives rise to the bridge output

$$V_y = \tfrac{1}{2}I[R(\alpha_+,\theta_+) - R(\alpha_-,\theta_-)], \quad (2)$$

where we have allowed for different magnetization orientations θ_+ and θ_- of the arms forming angles α_+ and α_- to the x-axis. The maximum bridge output is obtained when $\alpha_+ = -\alpha_- = \pi/4$ and is given by

$$V_y = \tfrac{1}{4}I\Delta\rho\tfrac{l}{wt}[\sin(2\theta_+) + \sin(2\theta_-)] \quad (3)$$

$$\equiv \tfrac{1}{4}V_{\rm pp}[\sin(2\theta_+) + \sin(2\theta_-)], \quad (4)$$

where we have defined the nominal peak-to-peak sensor output voltage $V_{\rm pp}$. Equation (4) is identical to the output voltage from a planar Hall effect sensor with cross-geometry except for the geometrical amplification factor l/w. Therefore, the above sensors have been termed planar Hall effect bridge (PHEB) sensors [4].

The values of θ_+ and θ_- can be found by minimizing the single domain energy density u for θ_+, α_+ and θ_-, α_-. Defining $\tilde{u} = u/(\mu_0 M_s)$, where μ_0 is the permeability of free space and M_s is the saturation magnetization of the material, we obtain the normalized energy density

$$\begin{aligned}\tilde{u} = &- H_{\rm y}\sin\theta - H_{\rm ex}\cos\theta - \tfrac{1}{2}H_{\rm K}\cos^2\theta \\ &- \tfrac{1}{2}H_{\rm s}\cos^2(\alpha-\theta)\end{aligned} \tag{5}$$

Here, H_y is the external magnetic field applied in the y-direction, $H_{\rm ex}$ is the exchange field due to a unidirectional anisotropy along $\theta = 0$, $H_{\rm K}$ is the anisotropy field due to a uniaxial anisotropy along $\theta = 0$ and $H_{\rm s}$ is the shape anisotropy field of the element. Denoting the demagnetization factors along and perpendicular to the element $N_\parallel$ and $N_\perp$, the shape anisotropy field is given by $H_{\rm s} = (N_\perp - N_\parallel)M_s$ [5]. For zero shape anisotropy $\theta_+ = \theta_- = \theta$. Equation (5) expands on previous work [4] where the shape anisotropy was not considered.

We will generally define the sensor low-field sensitivity S_0 by the relation

$$V_y = S_0 I H_y. \tag{6}$$

When the shape anisotropy is negligible ($H_{\rm s} = 0$), Eq.(5) can be minimized for small values of θ to give

$$S_0 = \frac{l}{w}\frac{\Delta\rho}{t}\frac{1}{H_{\rm K} + H_{\rm ex}}. \tag{7}$$

When the shape anisotropy is no longer negligible, it will give rise to a reduction of the low-field sensitivity compared to Eq.(7), whereas the peak-to-peak signal for small shape anisotropies will still be given by Eq.(3) [6].

3 EXPERIMENTAL

The top pinned PHEB sensor with the nominal stack Ta(3 nm)/$Ni_{80}Fe_{20}$(30 nm)/$Mn_{80}Ir_{20}$(20 nm)/ Ta(3 nm) (t = 56 nm) was grown by sputter deposition on a silicon substrate with a 1 μm thick thermal oxide and structured by lift-off. During deposition, a uniform magnetic field of $\mu_0 H_x$ = 20 mT was applied along the x-axis to define the easy direction and easy axis of magnetization in the permalloy layer. Contacts of Ti(10 nm)/ Pt(100 nm)/Au(100 nm)/ Ti(10 nm) were deposited by e-beam evaporation and defined by lift-off. The negative lithography process employed a reversal baking step at 120°C for 120 s on a hot plate in zero magnetic field.

The sensor dimensions in Figure 1 are w = 20 μm and l = 280 μm. The sensor was surrounded by magnetic stack with a 3 μm gap to reduce the shape anisotropy of the elements. The simple theory in Eq.(3) does not account for the effect of the corners of the stack. A finite element analysis of the sensor output assuming a single domain magnetization yielded the effective sensor aspect ratio l/w = 14.87, which is 6% higher than the nominal one, l/w = 14.

The magnetic properties of a continuous thin film with dimensions 3 × 3 mm^2 were characterized using a vibrating sample magnetometer (VSM) and values of $H_{\rm ex}$ and $H_{\rm K}$ were obtained from easy axis hysteresis loop measurements.

Values of the sheet resistances $\rho_\parallel/t$ and $\rho_\perp/t$ for the stack were obtained from resistance measurements on transmission line test structure in saturating magnetic fields applied parallel and perpendicular to the current.

During sensor measurements, the sensor was biased with an AC current of root-mean-square (RMS) amplitude $I_{\rm RMS} = 1/\sqrt{2}$ mA and frequency f = 65 Hz supplied by a Keithley 6221 precision current source. The first harmonic in-phase root-mean-square (RMS) signal $V_{y,\rm RMS}$ was measured using a Stanford Research Systems SR830 lock-in amplifier. We note that Eq.(4) also holds for the RMS values $V_{y,\rm RMS}$ and $I_{\rm RMS}$, we will therefore refer to the RMS values as V_y and I to simplify the notation below. The external field was generated by a custom electromagnet and monitored using commercially available Hall probes. The sensor characteristics were measured at temperatures from 25°C to 90°C regulated by means of a Peltier element and a platinum RTD to a stability better than 0.1°C. A reference measurement was performed at 25°C after every measurement at elevated temperatures to allow for the distinction between reversible and irreversible effects of heating.

4 RESULTS AND DISCUSSION

VSM measurements of the easy axis hysteresis loops yielded the values of exchange and anisotropy fields $H_{\rm ex}$ = 2.89(5) mT and $H_{\rm K}$ = 0.39(5) mT in good agreement with previous studies on a similar magnetic stack [7].

Electrical measurements on the transmission line structure carried out at room temperature yielded $\Delta\rho/t$ = 0.1296(1) Ω corresponding to an AMR ratio of 1.88% in agreement with previous studies [4]. Figure 2 shows the normalized sensor output V_y/I as function of the magnetic field applied in the y-direction measured at 25°C and 90°C. It is seen that the higher temperature leads to a reduced value of the peak-to-peak sensor output $V_{\rm pp}/I$ and also moves the peak position towards lower field values. The low-field sensitivity is observed to increase upon an increase of the temperature (see inset, Figure 2).

The solid lines in Figure 2 are fits obtained by minimizing Eq.(5) to obtain θ_+ and θ_- for the two orientations of the elements and inserting the result in Eq.(4). First, the fitting of all measurements was carried out with $V_{\rm pp}/I$, $H_{\rm ex}$, $H_{\rm K}$ and $H_{\rm s}$ as free parameters. As the

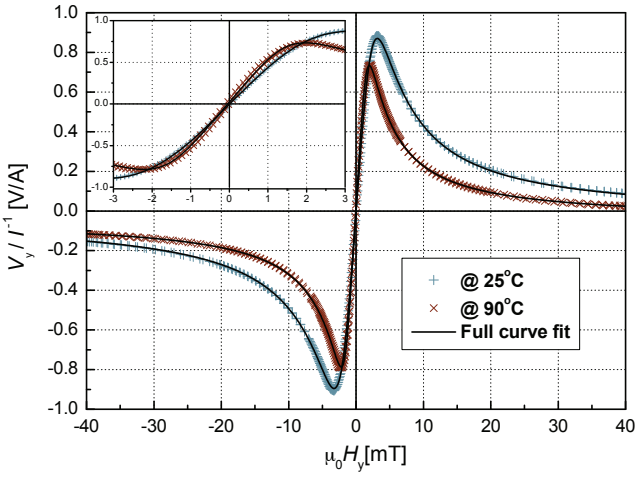

Figure 2: Sensor response V_y/I vs. applied magnetic field measured at 25°C and 90°C. The solid lines are curve fits obtained as described in the text. The inset shows a zoom-in on the low-field data.

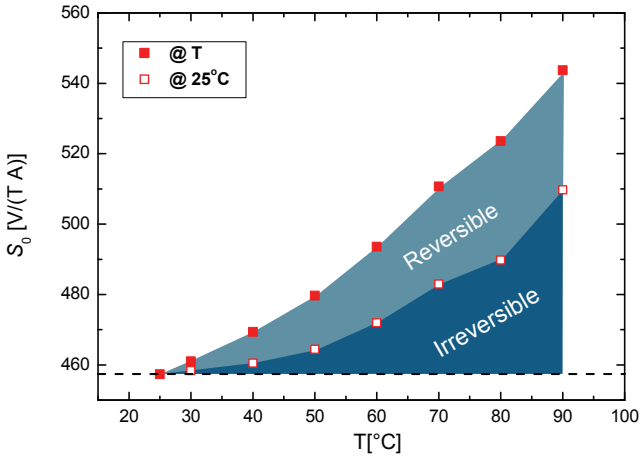

Figure 3: Low-field sensitivity vs. temperature extracted from the curve fits. Filled points are measured at T and open points are measured at 25°C after exposure to T.

value of H_s was found to only vary little between the fits, it was fixed to the average value $\mu_0 H_s = 0.97$ mT and all data were fitted again. In addition to the above parameters, we also allowed for offsets in the sensor output and the applied field. All fits were of a quality comparable to those in Figure 2.

From the fits of the data obtained at 25°C prior to heating, we obtain $H_{ex} = 2.69(2)$ mT, $H_K = 0.83(3)$ mT and $V_{pp}/I = 1.785(2)$ V/A. The value of H_{ex} obtained from the fit compares well with that obtained from the VSM measurements, whereas the value of H_K obtained from the fit is about twice that obtained from the VSM measurements. The latter observation is in agreement with previous studies [7] and the increase is attributed to effects of the sensor structure. The value of V_{pp}/I is expected to be given by $V_{pp}/I = (\Delta\rho/t)(l/w)$. Using the value of $\Delta\rho/t_{FM}$ obtained from the electrical measurements on the transmission line and the calculated effective aspect ratio of $l/w = 14.87$, we find $V_{pp}/I = 1.927(1)$ V/A, which is 8% higher than the value obtained from the fit. This deviation is likely due to demagnetization effects that modify the magnetization of the elements near their edges and corners.

Thus, we find that the single domain model provides a good description of the sensor response and that the parameters extracted from fitting compare well to independent measurements and hence can be considered reliable. Below, we will discuss the reversible and irreversible variation of S_0, V_{pp}, H_{ex} and H_K upon heating to a temperature T.

Figure 3 shows the low-field sensitivity S_0 extracted from the fits at temperature T and at 25°C after exposure to T as the slope between ± 0.15 mT. A comparison between the measurement carried out at temperature T and the reference measurement carried out at 25°C before exposure of the sensor to elevated temperatures shows the total change of S_0 with temperature. A comparison of the measurement carried out at 25°C after exposure to temperature T to the reference measurement shows the irreversible change of S_0 upon exposure to T. Hence, this approach enables us to distinguish between reversible and irreversible changes of the sensor response upon heating. The low-field sensitivity is found to increase about 17% when the temperature is increased from 25°C to 90°C and the observed sensitivity increase is in agreement with a previous study of cross-shaped PHE sensor with a similar magnetic stack [1]. Moreover, the results in Figure 3 show that more than 50% of the observed change of S_0 with increasing temperature is irreversible.

Figure 4 shows the corresponding temperature dependence of V_{pp}/I. We expect $V_{pp}/I = (\Delta\rho/t_{FM})(l/w)$ and hence the temperature dependence of V_{pp}/I will mirror that of $\Delta\rho$. Figure 4 shows that only a linear, reversible change of V_{pp}/I is observed upon increasing temperature. The change corresponds to a temperature coefficient of $-0.21\%/°C$, which is consistent with previous studies [1].

Figure 5 shows the total change and irreversible change of H_{ex} and H_K upon exposure to the temperature T. Both H_{ex} and H_K are found to decrease linearly with temperature when the temperature is increased with the temperature coefficients $-0.42\%/°C$ and $-0.68\%/°C$, respectively. Both parameters show irreversible changes of about the same absolute magnitude. The temperature coefficients of H_{ex} and H_K are larger than that of V_{pp}. Therefore, when these parameters are combined to form the ideal low-field sensitivity (for zero shape anisotropy) in Eq.(7), the decrease of $H_{ex} + H_K$ will

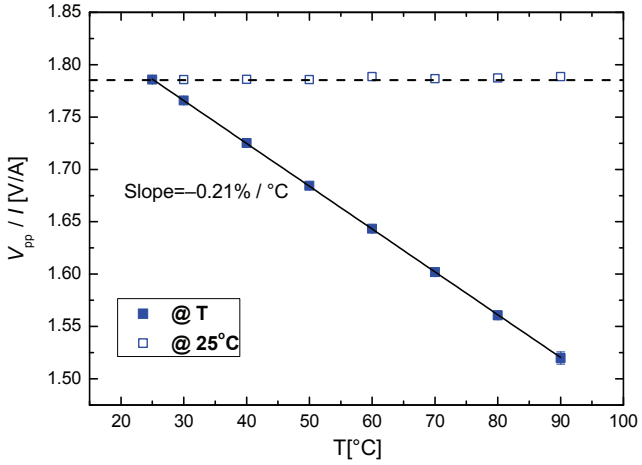

Figure 4: Peak-to-peak value of the sensor response vs. temperature extracted from the curve fits. Filled points are measured at T and open points are measured at 25°C after exposure to T. The full line is a linear fit.

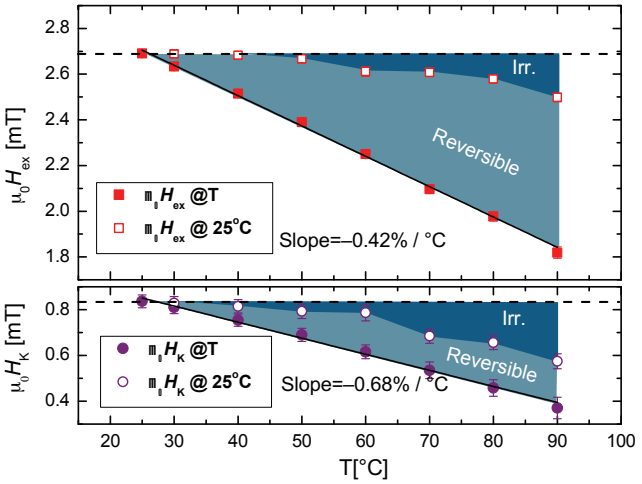

Figure 5: Exchange bias and anisotropy fields vs. temperature extracted from the curve fits. Filled points are measured at T and open points are measured at 25°C after exposure to T. The full lines are linear fits.

dominate over the decrease of V_{pp} causing the observed increase of S_0 with increasing temperature. The results also show that the irreversible change of S_0 can be solely attributed to irreversible changes of H_{ex} and H_{K} upon exposure to elevated temperatures.

Van Driel *et al.* [8] have studied top pinned structures with a similar stack by measuring hysteresis loops as function of temperature between room temperature and about 340°C. Their results for both the absolute and relative changes of H_{ex} agree well with our findings, but they did not distinguish between reversible and irreversible changes. Similar stacks have also been studied by Lorentz transmission electron microscopy [9] and magnetometry in combination with a structural characterization [10]. These studies attribute the changes of H_{ex} to changes of the magnetic domain structure of the antiferromagnet and explain the irreversible decrease of H_{ex} and H_{K} in terms of relaxation of frustrated interfacial spins due to the increased thermal energy [9, 10].

5 CONCLUSION

We have presented and demonstrated an effective technique to discriminate between reversible and irreversible changes in exchange-biased magnetic films and their effect on the sensitivity of planar Hall effect bridge magnetic field sensors upon exposure to temperatures between 25°C and 90°C. We have found that heating to 90°C results in a 10% irreversible increase and a 7% reversible increase of the low-field sensitivity relative to the initial value at 25°C. The observed total temperature variation of the thin film properties is consistent with the literature [9, 10]. The irreversible changes are attributed to irreversible reductions of the exchange and anisotropy fields due to thermal relaxation of the spin structure in the antiferromagnet. The results have a clear impact on the approach that should be taken to correct for temperature variations of the low-field sensitivity in applications where the sensors are exposed to elevated temperatures, e.g. in biological assays for magnetic biodetection.

Our future work will investigate the effect of low-temperature annealing that may stabilize the exchange interaction and reduce irreversible changes of the sensitivity upon exposure to elevated temperatures.

REFERENCES

[1] Damsgaard, C. D., et al. *Sens. Actuators, A* **156**(1), 103–108 (2009).
[2] Dalslet, B. T., et al. *Lab chip* **11**(2), 296–302 (2011).
[3] Persson, A., et al. *Sens. Actuators, A* **171**(2), 212–218 (2011).
[4] Henriksen, A. D., et al. *Appl. Phys. Lett.* **97**(1), 013507 (2010).
[5] Blundell, S. *Magnetism in condensed matter.* oxford master. Oxford University Press, (2001).
[6] Rizzi, G. et al. *Unpublished results* (2012).
[7] Damsgaard, C. D., et al. *J. Appl. Phys.* **103**(7), 07A302 (2008).
[8] van Driel, J., et al. *J. Appl. Phys.* **88**(2), 975 (2000).
[9] King, J. P., et al. *J. Phys. D: Appl. Phys.* **34**(4), 528–538 (2001).
[10] Geshev, J., et al. *J. Phys. D: Appl. Phys.* **44**(9), 095002 (2011).